

Received 9 July 2022, accepted 9 August 2022, date of publication 17 August 2022, date of current version 23 August 2022.

Digital Object Identifier 10.1109/ACCESS.2022.3199349

RESEARCH ARTICLE

Wireless Charging Constant Power Output System Based on LCC/S-S Self-Switching

ZHENG LI^{1,2}, (Member, IEEE), BO XIE¹, YIDING ZHU¹, MINGLEI TANG¹, HUIXIAN LIU¹,
XIAOQIANG GUO^{1,2}, (Senior Member, IEEE), AND HEXU SUN¹, (Senior Member, IEEE)

¹School of Electrical Engineering, Hebei University of Science and Technology, Shijiazhuang, Hebei 050018, China

²School of Electrical Engineering, Yanshan University, Qinhuangdao, Hebei 066004, China

Corresponding authors: Zheng Li (lzhfgd@163.com) and Hexu Sun (sunhxb@outlook.com)

This work was supported in part by the National Natural Science Foundation of China under Grant 51877070, Grant U20A20198, and Grant 51577048; in part by the Natural Science Foundation of Hebei Province of China under Grant E2021208008; in part by the Talent Engineering Training Support Project of Hebei Province under Grant A201905008; and in part by the National Engineering Laboratory of Energy-Saving Motor and Control Technique, Anhui University, under Grant KFKT201901.

ABSTRACT Conventional wireless charging systems cause output power fluctuations during the offset process, and a single topology can cause power reduction or a large impact on the wireless charging network as the coupling mutual inductance changes. For this reason, in this paper, by combining LCC-S and S-S topologies, the high output characteristics of the S-S topology network in the low coupling state and the high output characteristics of the LCC-S topology network in the protection and high coupling in the very low coupling, the power output in the offset state is greatly maintained by combining with the voltage regulation circuit. In this paper, firstly, the theoretical derivation of the working principle of the designed topology is carried out, then the mutual inductance variation range generated by the offset state of the coil is found through finite element simulation, and the accuracy of the theoretical derivation is verified by building a constant power output model of the self-switching system using matlab, and finally, an experimental platform for wireless power transmission is built, and the experimental results confirm that the system power can be maintained within a certain offset range. The output fluctuation is within 5%, which verifies the feasibility and realism of the design.

INDEX TERMS Wireless power transmission system, LCC-S topology, S-S topology, buck-boost network, constant power regulation.

I. INTRODUCTION

With the progress of science and technology and new environmental regulations, wireless power transmission (WPT) technology has attracted more attention and popularity because it eliminates the use of transmission lines in the traditional power supply mode, saves a lot of material resources, and has more significant advantages in reliability and security [1], [2], [3]. The couplers used in the design of the wireless charging system on both sides of the transceiver coil (Rx-coil and Tx-coil) belong to loose couplers. To reduce the transmission system loss and increase the system transmission power, the corresponding topologies are added on the primary

The associate editor coordinating the review of this manuscript and approving it for publication was Diego Masotti¹.

and secondary sides to compensate for the self-inductance of the coils. The four basic magnetically coupled resonant topologies commonly in use are series-serial (S-S), series-parallel (S-P), parallel-serial (P-S) and parallel-parallel (P-P) [3], [4], [5], [6]. The literature [7] analyzed the transmission characteristics of bilateral LCC-type resonant networks and confirmed that they have better anti-shift characteristics, but the system structure is complex and the compensation inductor is prone to coupling with the energy transfer coil. The literature [8] proposed a T/F variable structure compensation network based on the transmitter side, which achieves constant voltage/constant current mode switching by detecting and controlling the current on the transmitter side, and its structure is more fixed, and when the transmitter and receiver side of the WPT system produces an offset, whether,

in constant current or constant voltage mode, it will have a greater impact on the energy transmission of the WPT system. The literature [9] uses an LCC-N magnetically integrated compensation network to achieve energy transfer efficiency of more than 90% under both positive alignment and offset conditions, but its anti-offset property is only effective for unidirectional offset, which limits its development applications. The literature [10] proposed an LCC-C compensation network that achieves high-efficiency transmission at 8 mm close range, but its use conditions of low offset at close range also limit its development applications. In literature [11], a double-T capacitive energy transfer (CPT) system was designed to solve the problem of increasing the transient sudden change of the primary measurement current of the transmission system due to the sudden removal of the load end in the conventional S-S compensation network. In literature [12], the T-type compensation network is optimized to suppress power fluctuations within a certain tolerance range.

In order to keep the power output of the WPT system stable within a certain offset range, an LCC/S-S self-switching system is designed in this paper to reduce the power fluctuation by combining with a boost circuit to regulate the voltage. Firstly, the composition of the LCC/S-S self-switching system and the principle of pulse width modulation are introduced, then the mutual inductance change caused by coil offset is investigated by Ansys Maxwell, the validity of the design scheme is verified by Simulink in MATLAB, and finally the experimental platform is built to confirm the realism and feasibility of the design scheme.

II. WORKING PRINCIPLE ANALYSIS

Among the four basic compensation circuits in WPT system, the S-S type compensation network has been widely used because of its simple structure and good robustness, but when the mutual inductance decreases due to the offset of the transceiver side coil, its transmission power, and transmission efficiency will be significantly reduced, which has a greater impact on the transmission performance [13], [14]. In this paper, an LCC/S-S self-switching system is designed based on this compensation network, and by using the S-S compensation structure in the WPT system with low coupling and high power output, and the LCC-S compensation network with high coupling and high power output, the power fluctuation of WPT system in the offset state is reduced and the transmission performance of the system is improved.

The topology of the WPT self-switching system is shown in Figure 1. The transmitter side consists of a DC power supply U_{DC} , a full-bridge high-frequency inverter, a self-switching compensation network, and a transmitter coil, while the receiver side consists of a receiver coil, a rectifier, a filter capacitor C and a load R_L . The self-switching system changes the type of the compensation network by switching S_1 , S_2 , and S_3 . When switches S_1 and S_3 are closed and S_2 is broken, the topological compensation network of the

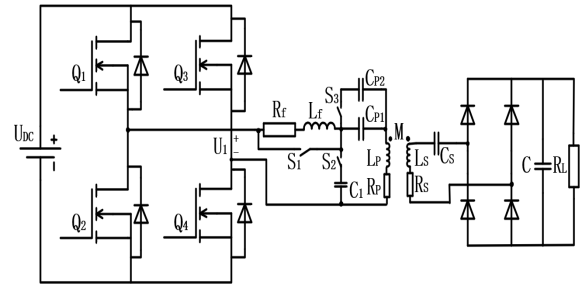


FIGURE 1. LCC/S-S self-switching WPT system.

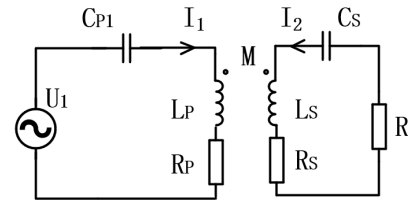


FIGURE 2. WPT system based on S-S type topology compensation network.

WPT system is S-S, and the compensation capacitor C_p on the transmitting side is composed of C_{p1} and C_{p2} . When the switch S_1 and S_3 are closed and S_2 is closed, the topology compensation network of the WPT system is LCC-S, at this time, the resistance and inductance of the series compensation coil are R_f and L_f , the series compensation capacitor is C_{p1} , and the parallel compensation capacitor is C_1 . The resistance and inductance of transceiver coil are R_p , L_p , R_s , and L_s , respectively. C_s is the series compensation capacitor of receiving side.

A. TOPOLOGY COMPENSATION PRINCIPLE ANALYSIS

1) S-S TYPE TOPOLOGY COMPENSATION PRINCIPLE ANALYSIS

When switch S_1 is closed and S_2 and S_3 are disconnected, the WPT system works in the S-S type topology compensation network state, whose topology is shown in Figure 2. The inverter output AC voltage is U_1 , and the currents flowing through the transceiver coils are I_1 and I_2 , respectively. When the losses of the rectifier bridge on the receiving side are not taken into account, the load resistance R_L is converted to the equivalent resistance of the rectifier bridge input as R [15], [16], whose value size satisfies equation (1):

$$R = \frac{8R_L}{\pi^2} \tag{1}$$

When the WPT system is in resonance, there is a supply voltage angular frequency ω equal to the angular frequencies ω_1 , ω_2 of the transceiver, i.e., equation (2) holds:

$$\omega = \omega_1 = \omega_2 = \frac{1}{\sqrt{C_{p1}L_p}} = \frac{1}{\sqrt{C_sL_s}} \tag{2}$$

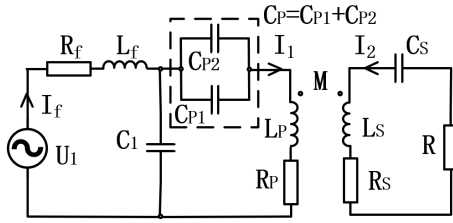


FIGURE 3. WPT system based on LCC-S type topology compensation network.

According to Kirchhoff’s voltage law (KVL), the loop equation is given in equation (3):

$$\begin{cases} U_1 = \left(R_P + j\omega L_P + \frac{1}{j\omega C_{P1}} \right) I_1 - j\omega M I_2 \\ -R I_2 = j\omega M I_1 + \left(R_S + j\omega L_S + \frac{1}{j\omega C_S} \right) I_2 \end{cases} \quad (3)$$

When the WPT system is in resonance, the transceiver side current is shown in equation (4):

$$\begin{cases} I_1 = \frac{(R_2 + R) U_1}{\omega^2 M^2 + R_1 (R_2 + R)} \\ I_2 = \frac{j\omega M U_1}{\omega^2 M^2 + R_1 (R_2 + R)} \end{cases} \quad (4)$$

At this point, the input power P_{in} , output power P_{out} and efficiency η of the system are shown in equation (5):

$$\begin{cases} P_{in} = \frac{(R_2 + R) U_1^2}{R_1 (R_2 + R) + (\omega M)^2} \\ P_{out} = \frac{R (\omega M)^2 U_1^2}{[R_1 (R_2 + R) + (\omega M)^2]^2} \\ \eta = \frac{R (\omega M)^2}{[R_1 (R_2 + R) + (\omega M)^2] (R_2 + R)} \end{cases} \quad (5)$$

From equation (4) and equation (5), it can be seen that when the resistance of the coil is ignored, the output power of the WPT system increases as the mutual inductance decreases, so the transmission characteristics can be used to reduce the sharp decrease of the transmission power under low coupling, but a protection circuit needs to be set to avoid the sharp increase of the current on the transmitting side when the load is removed, resulting in line burnout [17], [18].

2) LCC-S TYPE TOPOLOGY COMPENSATION PRINCIPLE ANALYSIS

When switch S_1 is disconnected and S_2 and S_3 are closed, the WPT system works in the LCC-S type topology compensation network state, and its topology is shown in Figure 3.

When the WPT system is in resonance, it satisfies equation (6):

$$\begin{cases} \omega L_P - \frac{1}{\omega C_P} = \frac{1}{\omega C_1} = \omega L_f \\ \omega L_S = \frac{1}{\omega C_S} \end{cases} \quad (6)$$

The voltage circuit equation is shown in equation (7):

$$\begin{cases} U_1 = (R_f + j\omega L_f) I_f + \left(R_P + j\omega L_P + \frac{1}{j\omega C_P} \right) I_1 + j\omega M I_2 \\ \left(R_P + j\omega L_P + \frac{1}{j\omega C_P} \right) I_1 + j\omega M I_2 = \frac{1}{j\omega C_1} (I_f - I_1) \\ -R I_2 = \left(R_S + j\omega L_S + \frac{1}{j\omega C_S} \right) I_2 + j\omega M I_1 \end{cases} \quad (7)$$

The input and output currents in the resonant state are shown in equation (8):

$$\begin{cases} I_1 = \frac{U_1}{j\omega C_1 R_f A} \\ I_2 = \frac{-M U_1}{C_1 R_f (R + R_S) A} \\ I_f = \frac{U_1}{R_f} - \frac{U_1}{(\omega C_1 R_f)^2 A} \end{cases} \quad (8)$$

where, A is shown in equation (9):

$$A = R_P + \frac{(\omega M)^2}{R + R_S} + \frac{1}{(\omega C_1)^2 R_f} \quad (9)$$

At this point, the output characteristics are shown in equation (10):

$$\begin{cases} P_{in} = \frac{U_1^2}{R_f} - \frac{U_1^2}{(\omega C_1 R_f)^2 A} \\ P_{out} = \frac{(M U_1)^2 R}{C_1^2 R_f^2 (R + R_S)^2 A^2} \\ \eta = \frac{(M U_1)^2 R}{A (R + R_S) [\omega^2 C_1^2 R_f (R + R_S) A - 1]} \end{cases} \quad (10)$$

From equation (8) and equation (10), it can be seen that when the coil resistance and the resistance of the series compensation inductor are ignored, the transmission power of the WPT system in this mode of operation decreases squared with the reduction of the mutual inductance, but the constant current characteristic of the transmitter side makes it widely used.

The design uses S-S topology to make the system compensate for power output at low coupling and set the threshold to achieve switching to the LCC-S topology network at too low a coupling coefficient to protect the WPT system circuit. The LCC-S topology is used to achieve stable and efficient energy transmission at high coupling coefficients, reduce the fluctuation of system transmission power, and increase the stability of the WPT system [19], [20]. The WPT system self-switching control flow is shown in Figure 4.

B. BOOST AND BUCK CIRCUIT CONTROL STRATEGY

Figure 5 shows the schematic diagram of the Buck-Boost chopper circuit. When the Mosfet tube is controlled to conduct and turn off, the relationship between its input and output voltage is shown in equation (11), where t_{on} is the on-time of

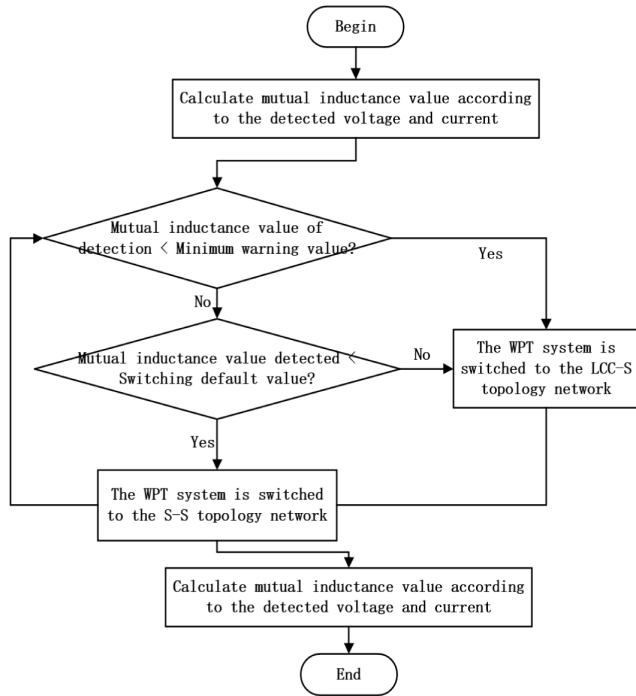


FIGURE 4. Self-switching control flow chart of WPT system.

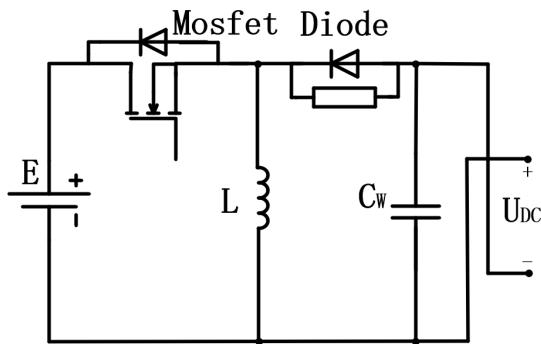


FIGURE 5. Schematic diagram of buck-boost chopper circuit.

the switch tube in one cycle T , and D is the duty cycle of the switch tube on. When $0 < D < 1/2$, it is in the step-down state; when $1/2 < D < 1$, it is in the step-up state [21], [22].

$$\begin{cases} D = \frac{t_{on}}{T} \\ U_{DC} = \frac{t_{on}}{t_{off}} E = \frac{D}{1-D} E \end{cases} \quad (11)$$

When the WPT system operates in the S-S topology state, it can be seen from equation (5) that the transmitted power is inversely proportional to the squared multiple of mutual inductance and proportional to the squared multiple of voltage, i.e., proportional to the squared duty cycle of the WPT system. And when operating in the LCC-S topology state, the transmission characteristics are exactly the opposite of the S-S type topology. For this reason, stable power output can be obtained by adjusting the duty cycle of the boost circuit

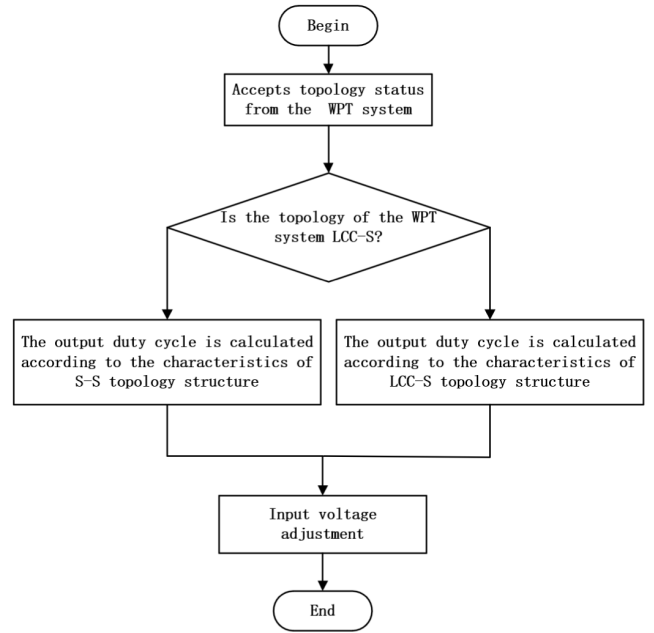


FIGURE 6. The voltage regulation flow chart of WPT system.

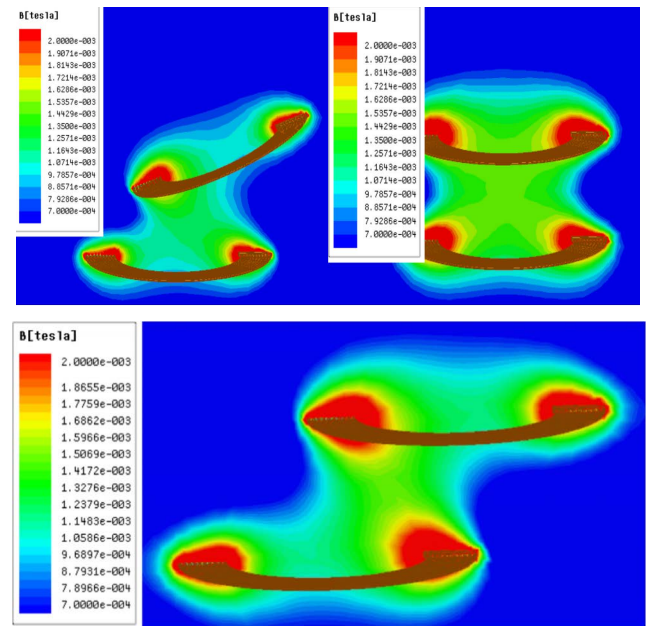


FIGURE 7. Magnetic field distribution in the offset state.

under different topology compensation networks, so that the WPT system can maintain a stable power output within a certain offset range. The voltage regulation flow chart of WPT system is shown in Figure 6.

III. SIMULATION ANALYSIS

A. OFFSET CHARACTERISTIC ANALYSIS

For simplicity, Figure 7 shows the magnetic field distribution of the 10-turn receiving coil under two cases of rotation around the axis and horizontal translation. As can be seen

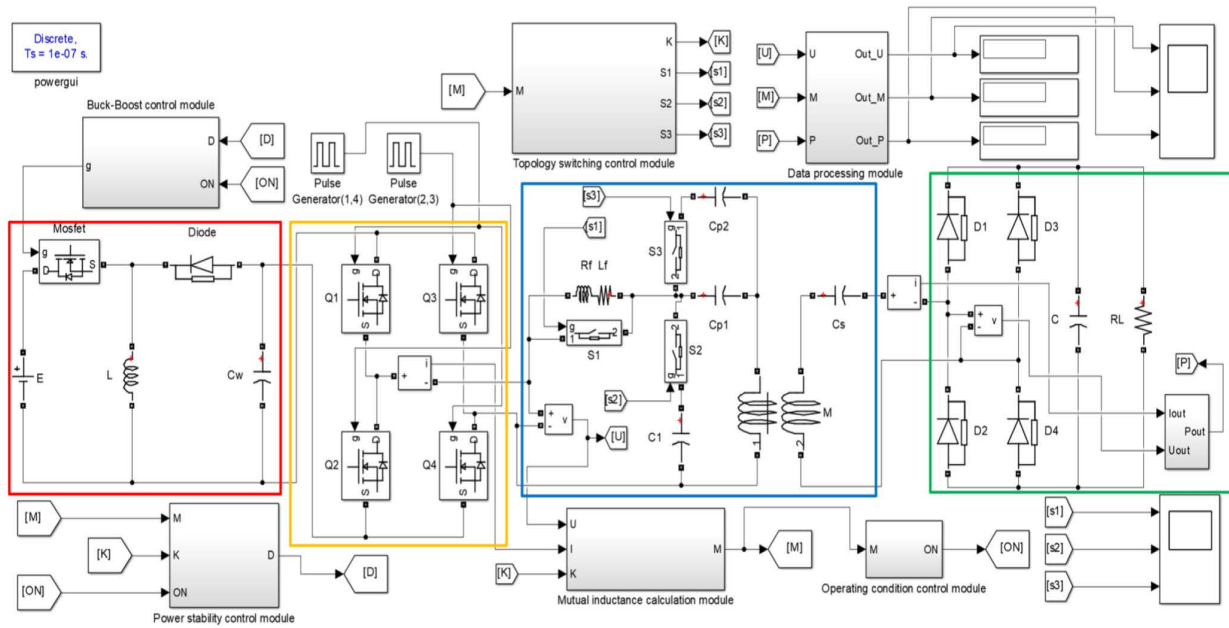


FIGURE 8. WPT self-switching constant power control system.

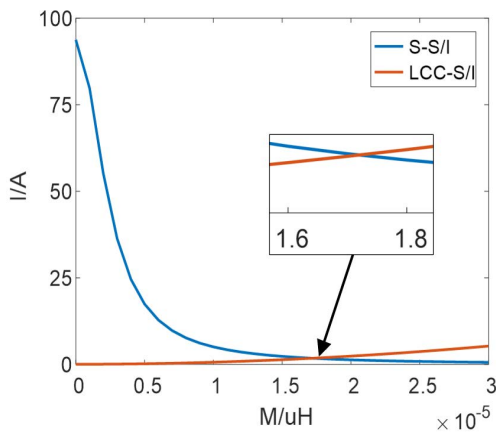


FIGURE 9. Primary-side current versus mutual inductance for different topology compensation networks.

from the simulation, the M of the coil varies in the range of $[0.44, 1.22]$ μH at this time, and the number of turns of the coil in the actual process is much larger than the simulated number of turns.

It is known that M is proportional to the product of the receiving and transmitting coils, and in order to combine the actual situation, the number of turns of the coil is set to 45 turns, which shows that in the actual process M of the coil varies around $[8.91, 24, 71]$ μH .

B. WPT CONSTANT POWER ANALYSIS

The analysis of the offset characteristics shows that the M generated during the offset of the WPT system varies in the range of $[8.91, 24, 71]$, and the WPT self-switching constant

power control system is built in Simulink according to the simulation parameters in Table 1 as shown in Figure 8. The WPT system is mainly composed of the main circuit and the control circuit. The box in the figure represents the main circuit. From left to right, it is composed of Buck-Boost chopper circuit, high-frequency inverter circuit, original and secondary side topology circuit, transceiver structure circuit, rectifier circuit and load. The package module includes the Buck-Boost control module, topology switching control module, data processing module, power stability control module, mutual inductance calculation module and operating condition control module. The main circuit and the control circuit cooperate with each other. When the transceiver structure of the wireless charging system is offset, the stable power output can be maintained by topological switching and input voltage regulation.

The intersection of the primary side current with the mutual inductance change curve in different operating modes of the self-switching system as the mutual inductance switching value, from Figure 9, it can be seen that the M at this time is about $17\mu\text{H}$. Let the stable power obtained from the secondary side be 50W . In order to avoid the communication between the primary and secondary sides and simplify the design of the WPT system, the current and voltage of the primary side are sent to the mutual inductance calculation module, and the calculated mutual inductance is sent to the topology switch control module to control the opening state of $S_1, S_2,$ and $S_3,$ and the topology of WPT system at this time is output by K ($K = 0$ means LCC-S; $K = 1$ means S-S); the other way is sent to the working condition control module to display the working state of WPT system and determine whether the WPT system is in normal

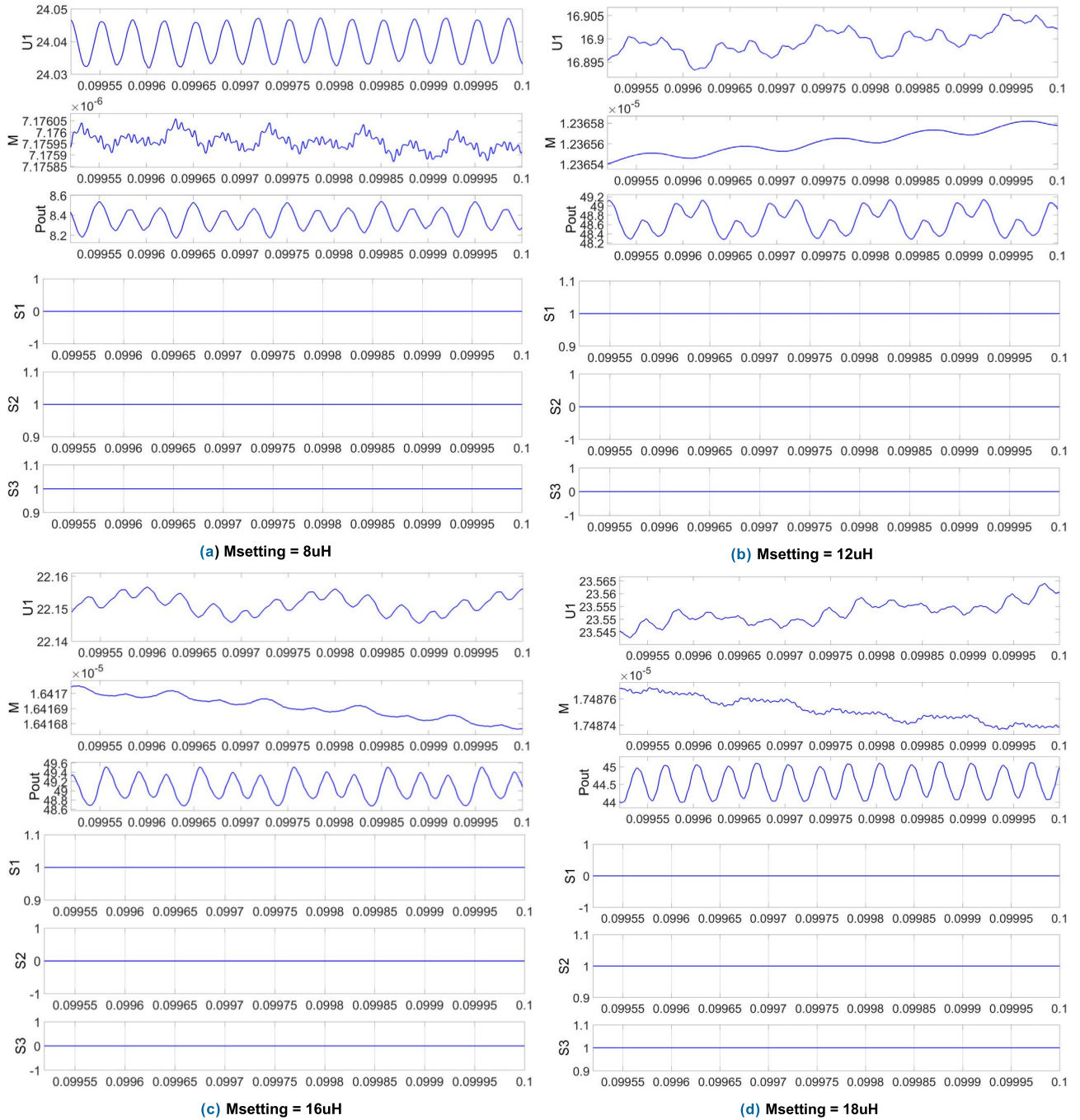


FIGURE 10. Input voltage U_1/V , measured mutual inductance M/H , output power P_{out}/W and switching operation state of the system under different M .

working state and whether the system input voltage needs to be adjusted to maintain constant power output. The power stabilization module sends the calculated duty cycle D to the boost control module and controls the input voltage by adjusting the trigger pulse signal of the Mosfet tube to realize the stable control of the WPT system with constant power. At the same time, the 10uH mutual inductance value is used as the low-coupling state protection output of the system, at which time the WPT system is judged to be in a

non-working state and the power stabilization regulation is stopped.

The simulation results of the WPT system in the vicinity of the mutual inductance switching value and the low coupling protection state are shown in Figure 10.

As can be seen from Figure 10, the switching of the topology from LCC-S to S-S is achieved during the 18uH and 16uH mutual inductance changes to reduce the impact of the offset, while the switching to LCC-S topology is achieved

TABLE 1. System simulation parameters.

Components	Parameter	Components	Parameter
E	15V	R_1	0.15Ω
L	1mH	L_1	51uH
C_w	100uF	R_2	0.15Ω
R_f	0.06Ω	L_2	50uH
L_f	20uH	C_s	70.12nF
C_{P1}	68.74nF	C	220uF
C_{P2}	44.35nF	R_L	10Ω
C_1	175.3nF	f	85kHz

TABLE 2. WPT system simulation results.

	S_1	S_2	S_3	U_1/V	M/uH	p_{out}/W	ON	
Set mutual inductance value $M_{setting}/uH$	6	0	1	1	24.02	6.19	4.33	0
	8	0	1	1	24.01	7.98	8.24	0
	12	1	0	0	16.89	12.37	48.88	1
	14	1	0	0	19.51	14.39	48.93	1
	16	1	0	0	22.16	16.42	49.04	1
	18	0	1	1	23.61	17.49	44.99	1
	20	0	1	1	21.31	19.39	44.99	1
	22	0	1	1	19.39	21.31	44.81	1
24	0	1	1	17.81	23.23	44.76	1	

during the 12uH and 8uH mutual inductance changes to protect the increase of the primary side current caused by the low coupling in the S-S state. Table 2 shows the operation of the designed system under different test conditions.

Due to the tube voltage drop and the existence of internal resistance, it will make the current of the system smaller than the calculated value, that is, the measured mutual inductance value under LCC-S is smaller than the real value, and the S-S state is larger. As can be seen from Table 2, the maximum error of the mutual inductance value is about 3%, and the maximum error of the transmission power is about 5W due to the accumulation of errors, which meets the design requirements.

IV. EXPERIMENTAL VERIFICATION

Figure 11 shows the overall device of wireless charging constant power transmission. DC voltage 10V not only provides

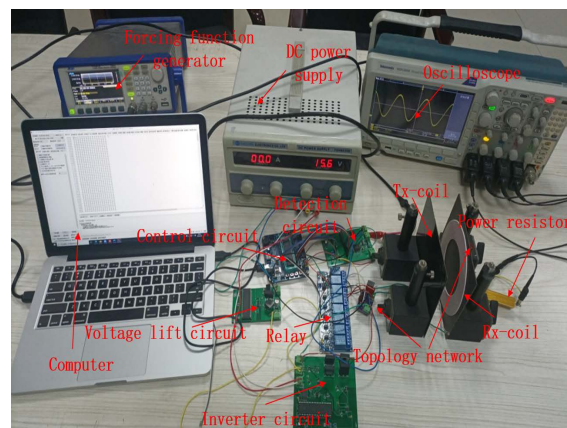


FIGURE 11. Wireless power transmission constant power control experimental device diagram.

TABLE 3. Topology experimental circuit device selection.

Components	Parameter	Components	Parameter
Tx-Coil Resistance R_1	0.6Ω	Transmitter series inductance L	22uH
Tx-coil inductance L_1	50uH	Transmitter series capacitor C_{P1}	68nH
Rx-Coil Resistance R_2	0.6Ω	Transmitter series capacitor C_{P2}	43nH
Rx-coil inductance L_2	50uH	Transmitter parallel capacitor C_1	180nH
Load Resistance R_L	8Ω	Receiver series capacitor C_s	68nH

the required power supply voltage, but also completes the voltage conversion through power supply chip H7805 to supply the chip, uses current detection module ACS712 to complete the detection of current, completes the measurement of input voltage through voltage divider resistor, and finally uses ADC0808 analog-to-digital converter chip to complete the signal acquisition. Through the STC89C52 to realize the mutual inductance and duty cycle calculation. The driving signal of the inverter circuit issued by the MCU is not only sent to the half-bridge driver module IR2014S through the HCPL optocoupler isolation module to drive the full-bridge inverter circuit; but also regulates the input voltage by controlling the conduction of MOSFET. The topology switching control signal sent by it controls the switching action of the relay [23], [24]. The relay module adopts electromagnetic mode, and its control characteristics of low voltage and low current make it have low power loss, which can realize effective switch of topology structure.

At the set frequency of 85kHz, the topology switching and power stability control are effectively completed. In order to reduce the experimental cost, the input voltage is controlled at 12V and the output power is steadily controlled at about 10W,

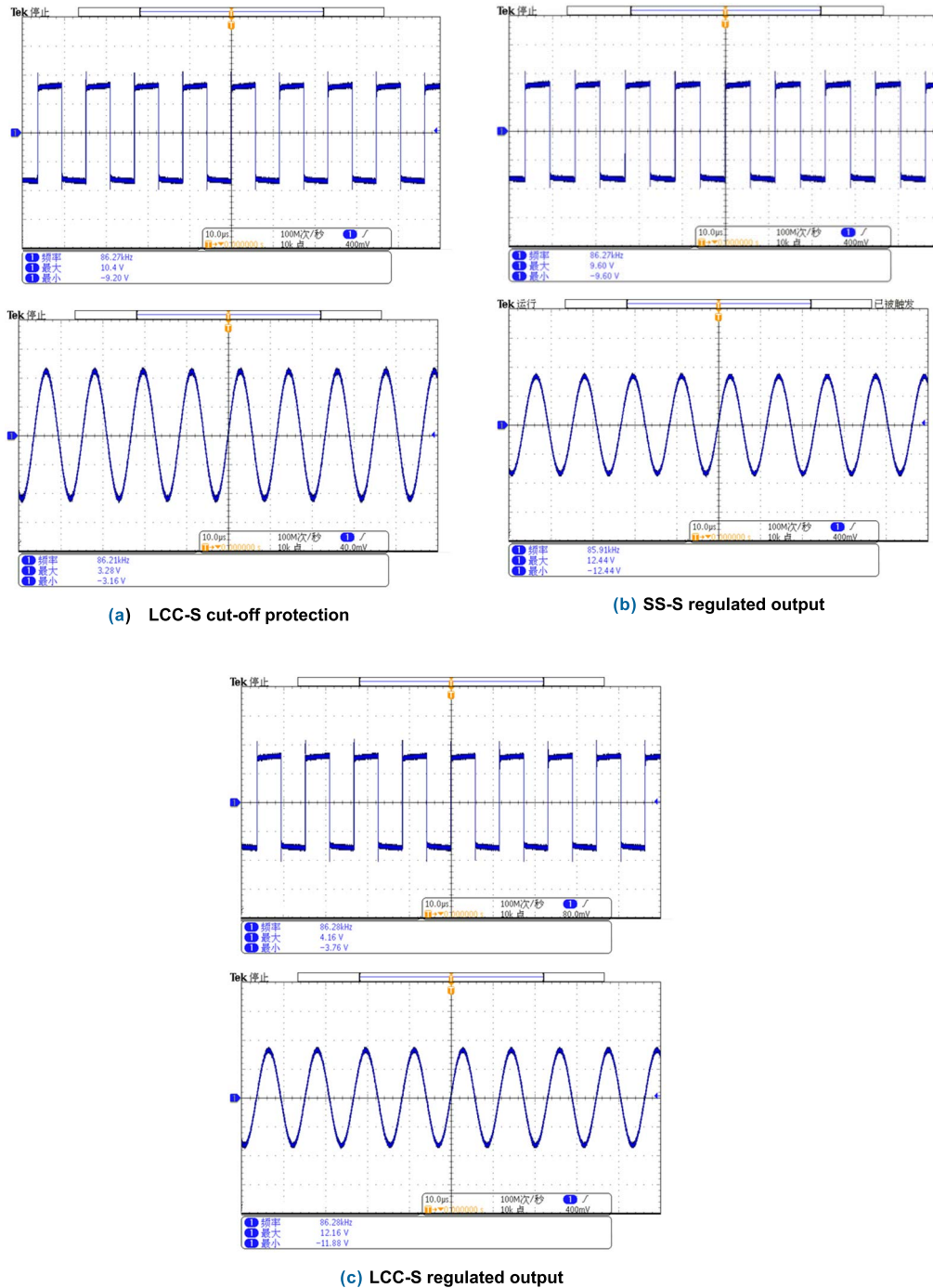


FIGURE 12. Oscilloscope input and output voltage waveforms under three different conditions.

and the topology circuit components are selected as shown in Table 3.

Figure 12 shows the input and output voltage waveforms of the oscilloscope under three different operating states of the wireless power transmission system, LCC-S cutoff protection, SS-S type and LCC-S steady power control. When the WPT system coupling is very small, the topology circuit switches to LCC-S to protect the system, and the input voltage

is locked to 10V at this time to facilitate the system to react to the change of cheap state in time. When the WPT system works normally, the system offset state is monitored by the voltage and current values detected at the transmitter, and the topology compensation method or the lift-off compensation is adjusted in time to maintain the stability of the system power.

Figure 13 illustrates the variation curve of the output power of the wireless power transmission system when the

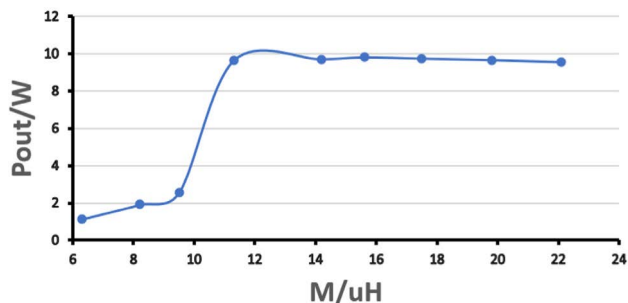


FIGURE 13. Power output at different offset states.

transceiver coil is shifted. From the figure, it can be seen that when the transceiver coil is offset to an excessive degree, the system is in standby mode for protection to cut off the input voltage regulation. When the transceiver coil is in the low or high coupling state, the WPT system makes the output power of the WPT system stable at about 10W by switching the topology compensation network and the voltage regulation module, and the fluctuation of the output power is controlled within 5%, which fully confirms the effectiveness of the design method.

V. CONCLUSION

At present, the design of topology compensation mode switching in WPT system mainly focuses on constant voltage and constant current control, and constant power output has significant advantages in solving capacity waste. Therefore, this paper designs a self-switching system based on LCC/SS-S topology. The power compensation for different offset states, combined with the buck-boost circuit, achieves power stability within a certain offset range. When the transceiver mechanism of the WPT system is offset, the mutual inductance is reduced too much, which proves that the system is in a non-working state at this time, and the WPT system stops working. When the mutual inductance is greater than 10uH, if the output of the WPT system does not reach the preset output at this time, the adjustment mechanism of the WPT will work to adjust the power. The experiment shows that through the power adjustment, the power fluctuation is controlled within 5%. It fully confirms the authenticity and feasibility of this research.

The method designed in this paper is based on the fixed WPT system. When the long-term use of the WPT system causes the parameters of the system components to change, the control mechanism of the system will also be affected. This is also the focus of the next research. The anti-interference ability of the WPT system is developed, and the WPT system is further improved.

REFERENCES

- [1] Z. Saiyao, "Research and application analysis of wireless charging technology for electric vehicles," *Commun. Power Technol.*, vol. 36, no. 7, pp. 133–134, 2019.
- [2] J. Dean, M. Coultis, and C. Van Neste, "Wireless sensor node powered by unipolar resonant capacitive power transfer," in *Proc. IEEE PELS Workshop Emerging Technol., Wireless Power Transf. (WoW)*, San Diego, CA, USA, Jun. 2021, pp. 1–5.
- [3] C. Xiao, K. Wei, F. Liu, and Y. Ma, "Matching capacitance and transfer efficiency of four wireless power transfer systems via magnetic coupling resonance," *Int. J. Circuit Theory Appl.*, vol. 45, no. 6, pp. 811–831, Jun. 2017.
- [4] G. Junling and Z. Qiang, "Research on SS-type compensation topology of electric vehicle wireless charging system," *J. Jiamusi Univ.*, vol. 39, no. 1, pp. 27–30, 2021.
- [5] Z. Yiming and W. Hui, "A compact wireless charging system for electric vehicles with strong offset resistance using hybrid topology," *Chin. Soc. Electr. Eng.*, vol. 42, no. 8, pp. 2979–2987, 2022.
- [6] L. Hongji and L. Ming, "Research on wide load range soft switch wireless charging compensation network based on class E inverter circuit," *Chin. Soc. Electr. Eng.*, pp. 1–14, Aug. 2022.
- [7] Y. Yang and W. Zhu, "Research on bilateral LCC resonance compensation network and electromagnetic safety of electric vehicle wireless charging system," *J. Xi'an Jiaotong Univ.*, vol. 55, no. 5, pp. 171–180, 2021.
- [8] T. Pingan and L. Jiawei, "Constant voltage/constant current wireless charging system based on T/F variable structure compensation network on the transmitter side," *J. Electrotechnical Technol.*, vol. 36, no. 2, pp. 248–257, 2021.
- [9] L. Zhimeng and T. Chengxuan, "Research on strong coupling wireless charging system based on LCC/N magnetic integrated compensation network," *Automot. Eng.*, vol. 43, no. 10, pp. 1528–1535, 2021.
- [10] L. Xuansong and P. Tinglong, "Design of wireless charging coil for cardiac pacemaker based on LCC-C," *Sensors Microsyst.*, vol. 40, no. 10, pp. 69–72, 2021.
- [11] Z. Liu, Y.-G. Su, Y.-M. Zhao, A. Patrick Hu, and X. Dai, "Capacitive power transfer system with double T-type resonant network for mobile devices charging/supply," *IEEE Trans. Power Electron.*, vol. 37, no. 2, pp. 2394–2403, Feb. 2022.
- [12] S. Li, L. Wang, Y. Guo, and C. Tao, "Optimization of T-type compensation network for a certain power fluctuation tolerance of the dynamic wireless power transmission," in *Proc. IEEE 4th Southern Power Electron. Conf. (SPEC)*, Singapore, Dec. 2018, pp. 1–5.
- [13] C. Cheng, Z. Zhou, W. Li, C. Zhu, Z. Deng, and C. C. Mi, "A multi-load wireless power transfer system with series-parallel-series compensation," *IEEE Trans. Power Electron.*, vol. 34, no. 8, pp. 7126–7130, Aug. 2019.
- [14] Z. Li, B. Xie, Y. Zhu, and H. Sun, "Optimal design of wireless power transfer system based on spherical motion device," *IEEE Access*, vol. 10, pp. 62661–62669, 2021.
- [15] Y. Li, J. Hu, F. Chen, S. Liu, Z. Yan, and Z. He, "A new-variable-coil-structure-based IPT system with load-independent constant output current or voltage for charging electric bicycles," *IEEE Trans. Power Electron.*, vol. 33, no. 10, pp. 8226–8230, Oct. 2018.
- [16] X. Ming and C. Xing, "A lightweight rectenna design," *Radio Commun. Technol.*, vol. 48, no. 2, pp. 366–370, 2022.
- [17] Y. Otomo and H. Igarashi, "A 3-D topology optimization of magnetic cores for wireless power transfer device," *IEEE Trans. Magn.*, vol. 55, no. 6, pp. 1–5, Jun. 2019.
- [18] G. Shengsheng, "Wireless charging system for electric vehicle lithium battery based on SS and PS composite resonant topology," *J. Mianyang Normal Univ.*, vol. 41, no. 2, pp. 23–29, 2022.
- [19] Y. Tian, Z. Zhu, L. Xiang, and J. Tian, "Vision-based rapid power control for a dynamic wireless power transfer system of electric vehicles," *IEEE Access*, vol. 8, pp. 78764–78778, 2020.
- [20] V. Shevchenko, S. Member, O. Husev, and S. Member, "Compensation topologies in IPT systems: Standards, requirements, classification, analysis, comparison and application," *IEEE Access*, vol. 7, pp. 120559–120580, 2019.
- [21] Z. Zhou, W. Li, C. Cheng, C. Wang, Z. Deng, and C. Mi, "A wireless power transfer system powering multiple gate drivers in a modular multilevel converter," in *Proc. IEEE PELS Workshop Emerg. Technologies: Wireless Power Transf. (WoW)*, London, U.K., Jun. 2019, pp. 401–405.
- [22] H. Yiwen and C. Bowen, "Design of synchronous rectification BUCK DC-DC regulated switching power supply," *Modern Electron. Technol.*, vol. 45, no. 4, pp. 94–100, 2022.
- [23] N. Ayir, T. Riihonen, M. Allen, and M. F. T. Fierro, "Waveforms and end-to-end efficiency in RF wireless power transfer using digital radio transmitter," *IEEE Trans. Microw. Theory Techn.*, vol. 69, no. 3, pp. 1917–1931, Mar. 2021.
- [24] H. Zhu, B. Zhang, and L. Wu, "Output power stabilization for wireless power transfer system employing primary-side-only control," *IEEE Access*, vol. 8, pp. 63735–63747, 2020.



ZHENG LI (Member, IEEE) was born in Shijiazhuang, Hebei, China, in 1980. He received the B.Sc. and Ph.D. degrees in electrical engineering and power electronics and electric drive from the Hefei University of Technology, Hefei, China, in 2002 and 2007, respectively

Since 2007, he has been a Lecturer, an Associate Professor, and a Professor with the School of Electrical Engineering, Hebei University of Science and Technology. From July 2013 to July 2014,

he has been a Visiting Scholar and a part-time Faculty with the College of Engineering, Wayne State University, USA. He is the author of more than 240 published articles. His current research interests include design, analysis, and control of novel motors and actuators, intelligent control, and power electronics.

Dr. Li is an Active Reviewer of the IEEE TRANSACTIONS ON INDUSTRIAL ELECTRONICS, the IEEE TRANSACTIONS ON ENERGY CONVERSION, the IEEE TRANSACTIONS ON MAGNETICS, and *Electric Power Components and Systems*.



BO XIE was born in Langfang, China, in 1997. He received the bachelor's degree in electrical engineering and automation from the Hebei University of Science and Technology, in 2020, where he is currently pursuing the master's degree.

He is also a Graduate Student with the Hebei University of Science and Technology. His research interests include wireless power transmission and motor drive.



YIDING ZHU was born in Shijiazhuang, China, in 1995. He received the bachelor's degree in automation from the Chongqing University of Technology, in 2018. He is currently pursuing the master's degree with the Hebei University of Science and Technology.

He is also a Graduate Student at the Hebei University of Science and Technology. His research interests include the research of special motors, and vibration and noise suppression of linear motors.



MINGLEI TANG was born in Handan, China, in 1996. He received the bachelor's degree in electrical engineering and automation from the Polytechnic College, Hebei University of Science and Technology, in 2020. He is currently pursuing the master's degree with the Hebei University of Science and Technology.

He is also a Graduate Student with the Hebei University of Science and Technology. His research interest includes wireless power transmission.



HUIXIAN LIU was born in Ninjin, China, in 1984. She received the Ph.D. degree in control theory and control engineering from Southeast University, Nanjing, China, in 2012.

Since 2011, she has been with the School of Electrical Engineering, Hebei University of Science and Technology, where she is currently an Associate Professor. Her research interests include nonlinear system control, and predictive control with applications to ac motors.



XIAOQIANG GUO (Senior Member, IEEE) received the B.S. and Ph.D. degrees in electrical engineering from Yanshan University, Qinhuangdao, China, in 2003 and 2009, respectively.

He was a Postdoctoral Fellow with the Laboratory for Electrical Drive Applications and Research, Ryerson University, Toronto, ON, Canada. He is currently a Professor with the Department of Electrical Engineering, Yanshan University. He has authored or coauthored more than 80 technical

articles and in addition to 11 patents. His current research interests include high-power converters and ac drives, electric vehicle charging station, and renewable energy power conversion systems. He is a Senior Member of the IEEE Power Electronics Society and the IEEE Industrial Electronics Society. He is an Associate Editor of the *China Power Supply Society (CPSS) Transactions on Power Electronics and Applications*, *Journal of Power Electronics*, and *IET Power Electronics*.



HEXU SUN (Senior Member, IEEE) received the Ph.D. degree in automation from Northeastern University, Shenyang, China, in 1993. He has been a Professor with the School of Control Science and Engineering, Hebei University of Technology, Tianjin, China, and the School of Electrical Engineering, Hebei University of Science and Technology, Shijiazhuang, China. He has authored five books and more than 130 journals and conference papers, and holds 13 U.S. patents and five computer software copyrights.

His current research interests include robotics and complex engineering systems. He was a recipient of many prestigious national awards from China. He has been the Director in many societies and committees in China. He is currently the invited plenary speaker and a general co-chair of many international conferences.

...